Supplemental information

Supplemental Figures 1-6

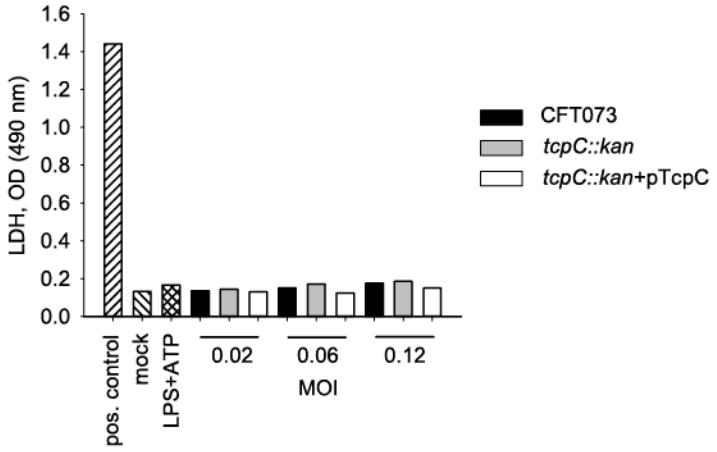

Figure S1: Infection of BMDM with CFT073 strains is not toxic. Cytotoxicity was determined using the lactate dehydrogenase (LDH) release assay. Culture supernatants of cells described in Fig. 1A were analyzed for LDH release. Lysed cells were used as positive control. Data represent mean of two individual cultures.

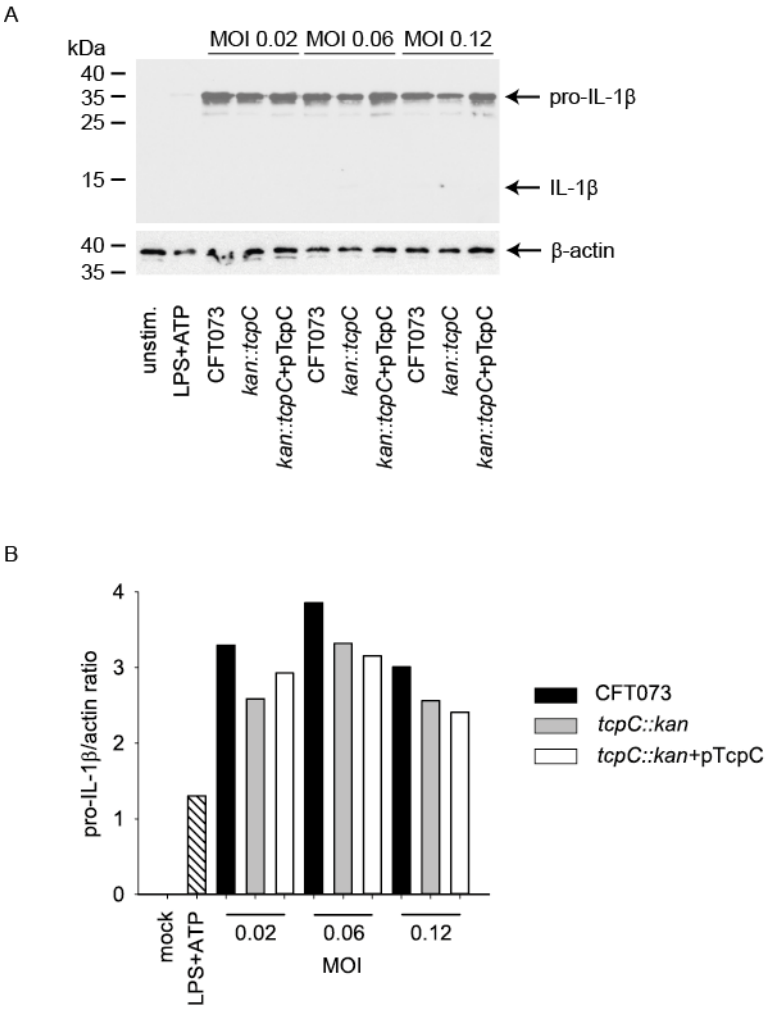

Figure S2: Infection of BMDMs with CFT073 strains induced pro-IL-1β expression. Pro-IL-1β and β-actin expression was quantified by densitometry using ImageJ and the Western blot shown in Fig. 1C. To quantify pro-IL-1β a film with a short exposure time was used (A). The ratio of band densities of pro-IL-1β and β-actin is shown in (B).

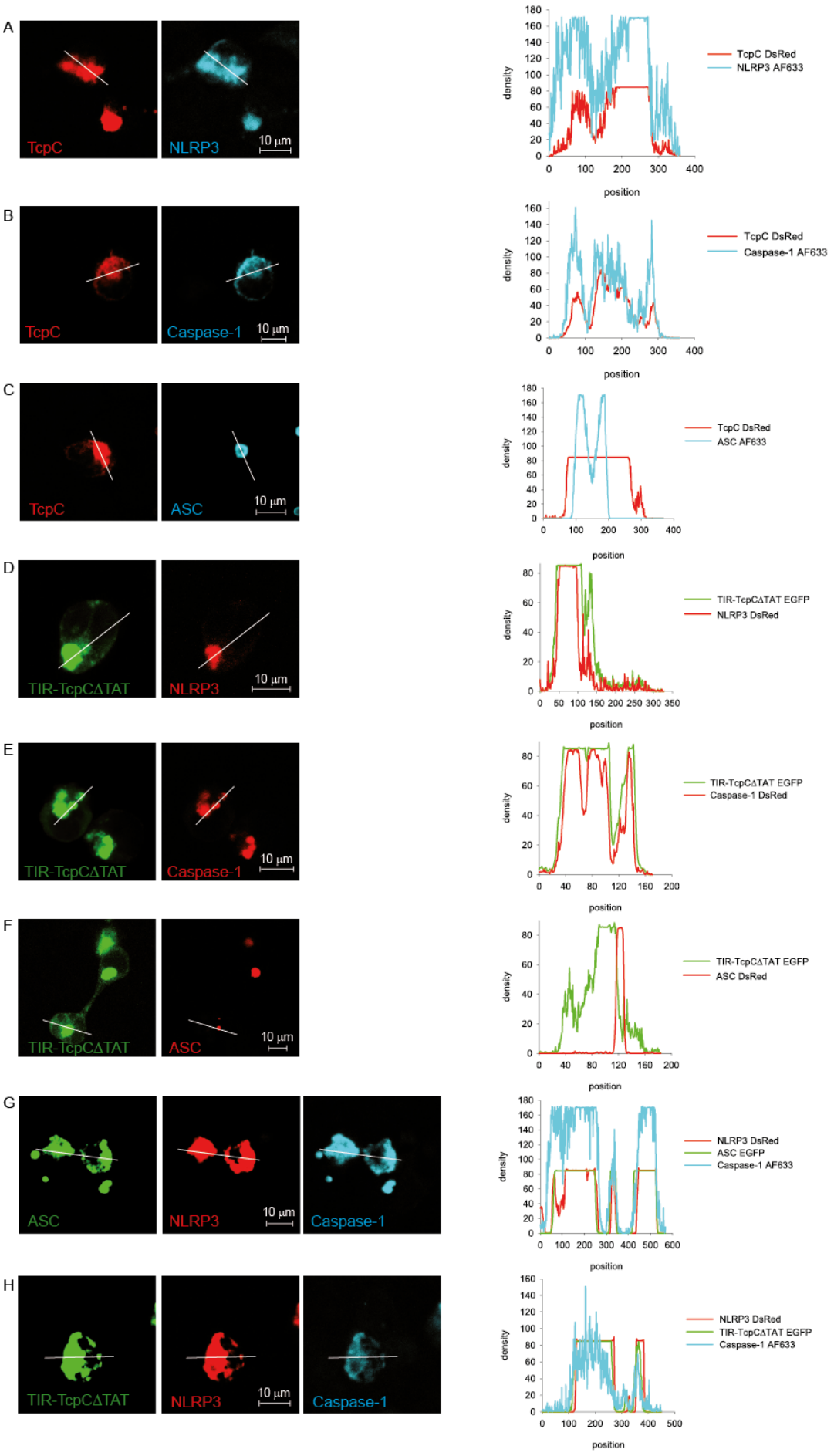
A
TcpC
NLRP3
10 µm
density
position
TcpC DsRed
NLRP3 AF633
B
TcpC
Caspase-1
10 µm
TcpC DsRed
Caspase-1 AF633
C
TcpC
ASC
10 µm
TcpC DsRed
ASC AF633
D
TIR-TcpCΔTAT
NLRP3
10 µm
TIR-TcpCΔTAT EGFP
NLRP3 DsRed
E
TIR-TcpCΔTAT
Caspase-1
10 µm
TIR-TcpCΔTAT EGFP
Caspase-1 DsRed
F
TIR-TcpCΔTAT
ASC
10 µm
TIR-TcpCΔTAT EGFP
ASC DsRed
G
ASC
NLRP3
10 µm
Caspase-1
NLRP3 DsRed
ASC EGFP
Caspase-1 AF633
H
TIR-TcpCΔTAT
NLRP3
10 µm
Caspase-1
NLRP3 DsRed
TIR-TcpCΔTAT EGFP
Caspase-1 AF633

Figure S3: Quantification of the colocalization of TcpC with NLRP3 or caspase-1. Confocal images presented in Fig. 3 were quantitatively analyzed by measuring the expression densities along the indicated white line in each graph using ImageJ. Densitometry results are presented in the graphs on the right of A-H. The x-axis of each graph represents the position of each point along the indicated white line, the y-axis the densitometry value of each point in arbitrary units. While the densitometry curves of TcpC and NLRP3 (A) or TcpC and caspase-1 (B) were almost of identical shape, this was not the case for TcpC and ASC (C). Similarly, densitometry curves of TIR-TcpCΔTAT and NLRP3 (D) or TIR-TcpCΔTAT and caspase-1 (E) were again almost identical, this was not the case for TIR-TcpCΔTAT and ASC (F).

Quantitative analysis of the expression of ASC, NLRP3 and caspase-1 revealed similar densitomety curves for all three molecules (G). An identical result was obtained when ASC was replaced with TIR-TcpCΔTAT (H).

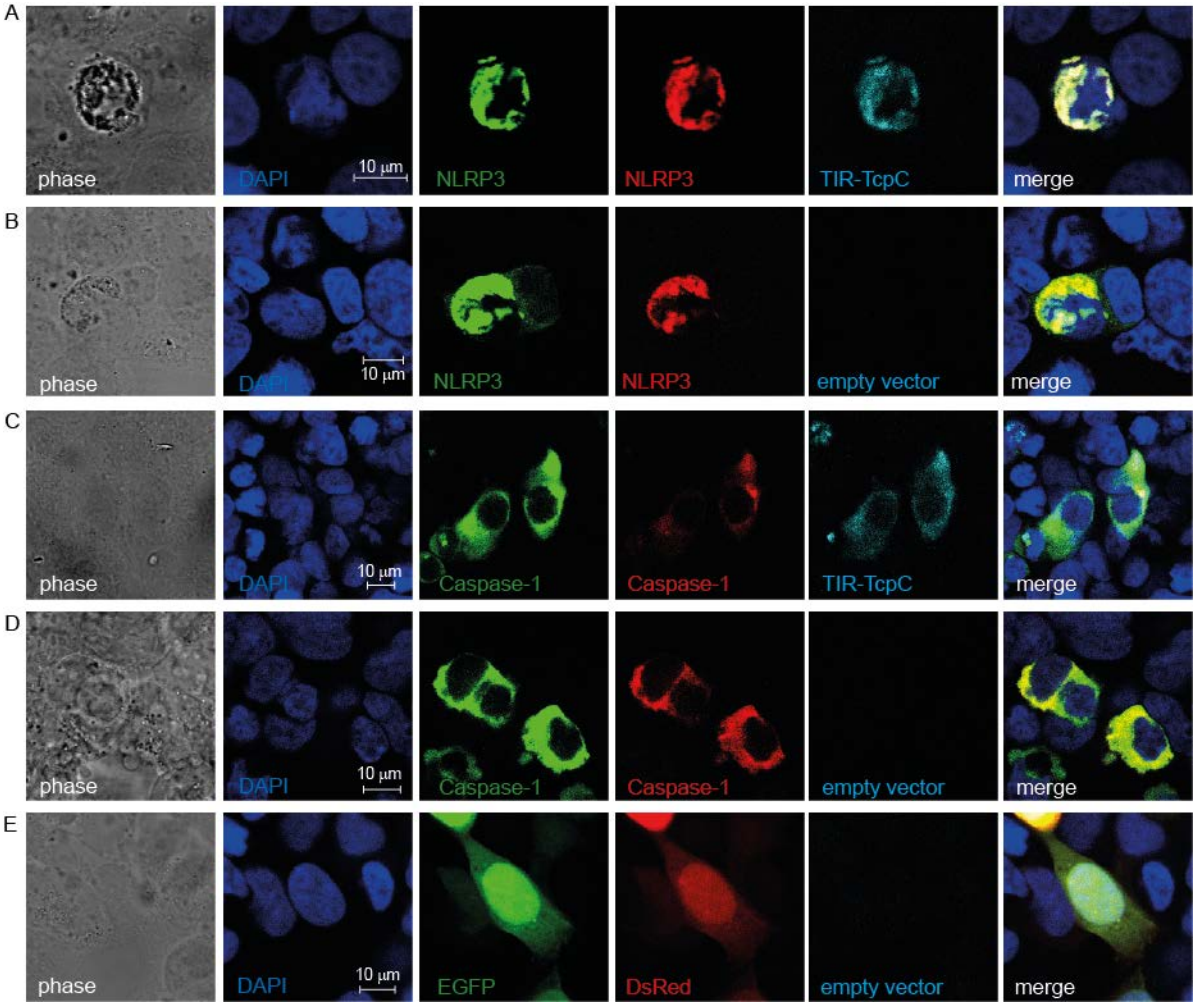

Figure S4: Colocalization of TIR-TcpC with NLRP3 or caspase-1. Flag-tagged TIR-TcpC was cotransfected with NLRP3 (A) or caspase-1 (C) which were double-labeled with EGFP and DsRed. Thus, the labeling of the colocalizing proteins was reversed in comparison to Fig. 3. Empty vector encodes only for the flag-tag and served as negative control (B, D). In (E) cells were transfected with a vector encoding only EGFP and DsRed and served as another negative control.

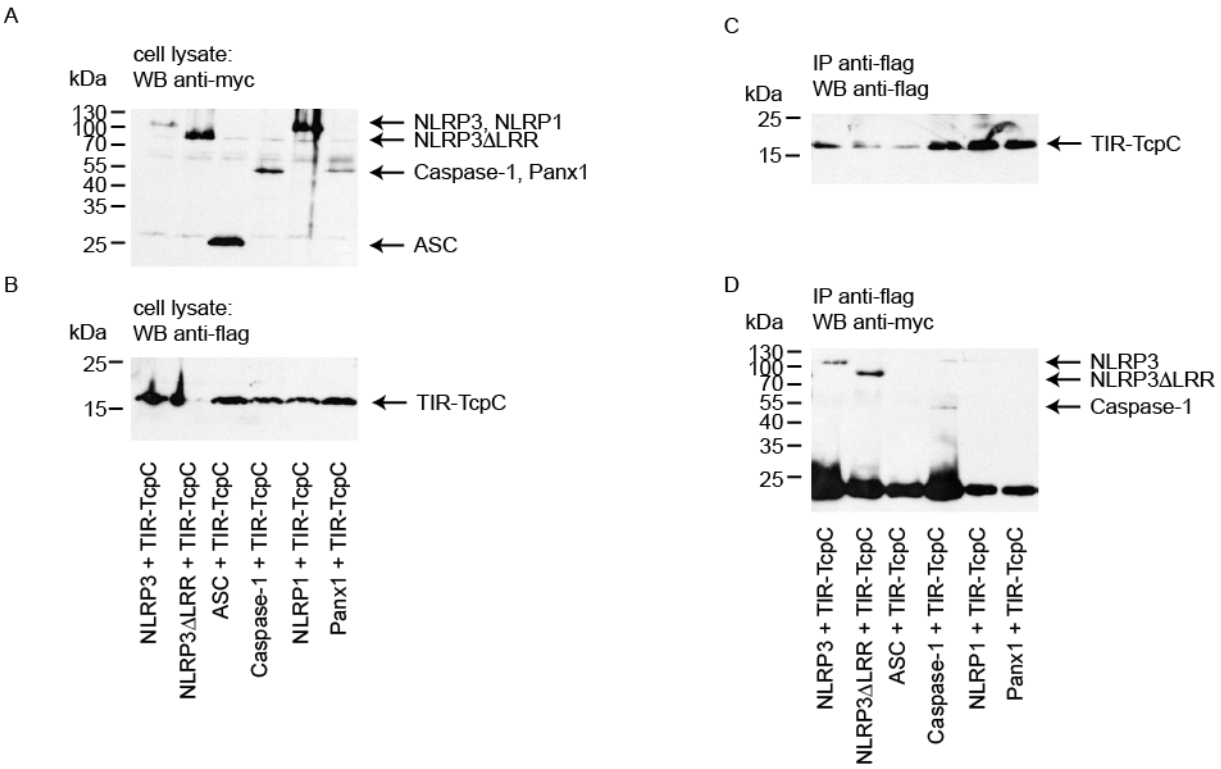

Figure S5: TcpC failed to bind NLRP1 or Pannexin-1. (A-D) We transiently transfected HEK293 cells with flag-labeled TIR-TcpC together with myc-tagged NLRP3, myc-tagged NLRP3ΔLRR, myc-tagged caspase-1, myc-tagged ASC, myc-tagged NLRP1 or myc-tagged Pannexin-1 (Panx1). (A, B) expression of inflammasome proteins and TIR-TcpC in cell lysates, (C) Anti-FLAG affinity beads were used to immunoprecipitate flag-tagged TcpC. (D) Bound myc-tagged proteins were visualized using anti-myc antibodies.

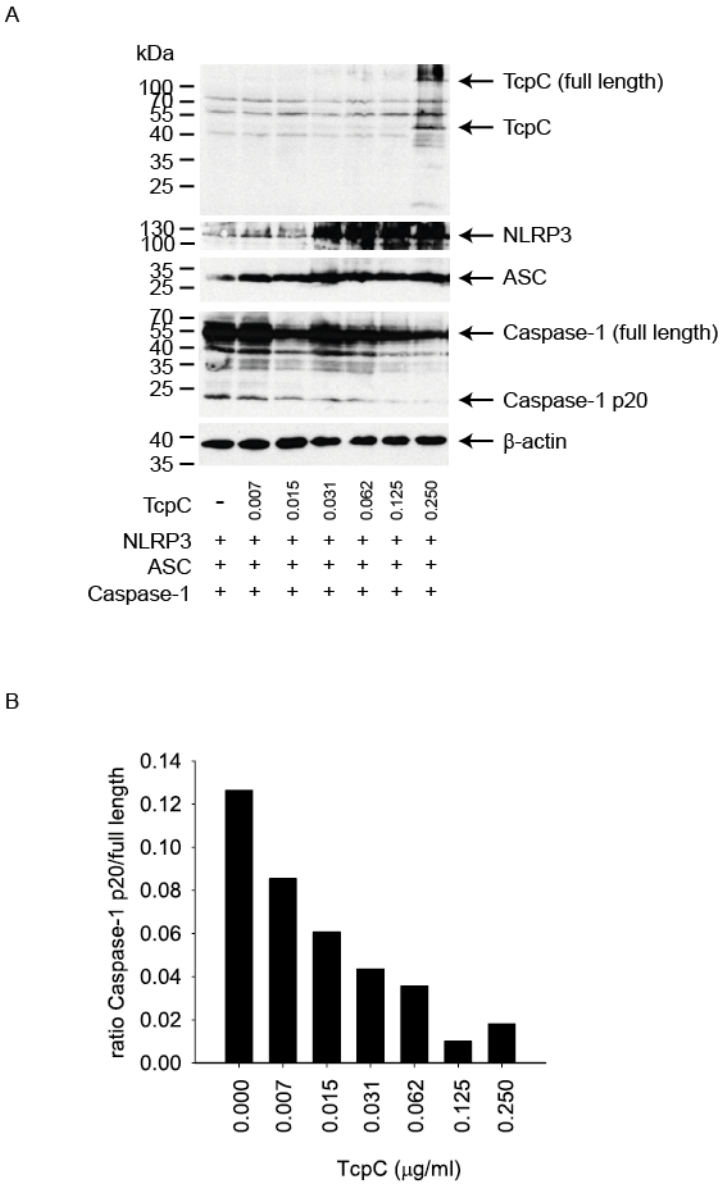

Figure S6: TcpC impairs activation of caspase-1. (A) We transiently transfected HEK293 cells ($1x10^6$/2 ml) with titrated amounts of EGFP/DsRed double-labeled TcpC (0.00-0.25 µg/ml) together with myc-labeled NLRP3 (0.75 µg/ml), flag-labeled ASC (0.1 µg/ml), flag-labeled caspase-1 (0.75 µg/ml) as indicated. The total transfected DNA amount was kept constant by addition of an empty vector to 1.85 µg DNA/ml. TcpC was visualized by an anti-EGFP, caspase-1 by an anti-caspase-1 p20, ASC by an anti-flag antibody. β-actin served as loading control. (B) The density of caspase-1 p20 and full length caspase bands were quantified using ImageJ and the caspase-1 p20/full length ratio was calculated.